Available online at www.sciencedirect.com
SCIENCE DIRECT®
Physica A 339 (2004) 267–284
PHYSICA A
www.elsevier.com/locate/physa

Remaining coverage in associative desorption process

O. Furlong, S. Manzi, G. Costanza, V.D. Pereyra*

Laboratorio de Ciencias de Superficie y Medios Porosos, Departamento de Física, Universidad Nacional de San Luis, CONICET, Chacabuco 917, San Luis 5700, Argentina

Received 4 July 2003; received in revised form 20 February 2004

Abstract

In this paper the kinetic of dissociative adsorption of dimers followed by associative desorption is analyzed. The coupled differential equations which describe the kinetics of the process were obtained by applying the so-called local evolution rules. Particular interest presents the irreversible desorption process. In fact, given that desorption proceeds from the reacting nearest-neighbor monomers, a remaining coverage results from those isolated particles when the mobility is neglected, therefore, the resulting configuration can be considered as a jamming state of the system. The exact solution for the remaining coverage is obtained in one-dimensional chain, where the effect of the lateral interactions are also included. The two-dimensional case is analyzed by using Monte Carlo simulation. The equilibrium solutions and the thermal desorption spectra are also studied.

PACS: 82.40.F; 82.65.J, Y; 82.20

Keywords: Adsorption kinetics; Associative desorption; Surface reactions

1. Introduction

Heterogeneous catalysis involves different steps like adsorption, surface diffusion, reaction and desorption. These processes are largely analyzed in the surface science and many of them are by now well understood [1–4]. In fact, development of new experimental techniques, such as field ion microscopy or scanning tunneling microscopy, has opened up the possibility to monitor chemical reactions on surfaces of metal

* Corresponding author. Tel.: +54-2652423789; fax: +54-2652430224.
E-mail address: vpereyra@unsl.edu.ar (V.D. Pereyra).

0378-4371/$ - see front matter
doi:10.1016/j.physa.2004.03.018

catalysts in real time with almost atomic resolution [1,2]. Thus, the behavior of particles on surfaces, even reactive particles become directly observable. Motivated by these experimental findings, new theoretical approach as well as numerical simulations have been proposed [3,4].

One of the various steps involved in heterogeneous catalysis is the adsorption process. The experimental evidence shows that in most of the catalytic surface reactions, larger molecules dissociate after adsorption. States like these existing over empty sites are called intrinsic precursor states [5,6]. The most common example of such precursors are weakly bound molecular states for diatomic molecules on metal surfaces, from which dissociation into strongly bound atomic adsorption may occur.

Besides that, in many catalytic reactions single atoms associate in the surface to desorb as molecular species. The kinetic of associative desorption has been largely studied by means of a great number of experimental techniques [1,2], as well as using different theoretical approaches [3] and computer simulations [4]. There are several examples where associative desorption is present, particularly, those catalyzed reactions that follow the Langmuir–Hinshelwood mechanism, for instance, the oxidation of carbon monoxide and the reaction between NO and CO over single-crystal catalyst. In the first one, the CO reacts with a O atom to form a CO_2, which desorb from the surface, while in the second reaction the product is N_2 and CO_2 which desorb to the gas phase.

Dissociative adsorption, associative reactions, and desorption of simple molecules concomitant with the metal surface restructuring are of particular interest. These processes have been discussed for reactions involving H–H, C–H or C–C bond breaking on stepped and kinked crystal faces of platinum [7]. These reactions have been analyzed by means of theoretical approach and Monte Carlo simulations [8,9]. However, some aspects of the process are still unclear and deserve to be analyzed, particularly the adsorption–desorption kinetics.

Here, the kinetic of dissociative adsorption of dimers followed by associative desorption was studied. The process is described by using the one-dimensional lattice gas model, particularly, the evolution equations of the observable are derived throughout the so-called local evolution rules [10–12]. The equilibrium properties, adsorption isotherms and nearest-neighbor correlation are derived from the kinetic equations.

The irreversible kinetics is also considered. Particularly, when the only process allowed in the surface is the molecular desorption, there is a remaining coverage due to the isolated atoms on the substrate. This coverage can be removed by increasing temperature or by surface diffusion. However, for certain range of temperature, the remaining coverage can be considered as an irreversible state or jamming state of the system.

Thermal desorption is also analyzed in one- and two-dimensional lattices, for different lateral interactions. The two-dimensional lattices with repulsive lateral interactions, where the system undergoes a second-order phase transition, are of special interest.

The rest of the paper is organized as follows: In Section 2, the model is introduced and the kinetic equations, which describe the process, are derived. In Section 3, different aspects of the kinetics are discussed, in the first place the reversible kinetics, where the equilibrium properties are derived from the evolution equations and an exact form for

the one-dimensional isotherms are obtained. Then, the irreversible kinetics are studied. The exact solution for the irreversible isothermal desorption is obtained, calculating the remaining coverage as a function of the initial coverage and its dependence with lateral interactions. Finally, the thermal programmed desorption (TPD) spectra are obtained from the kinetic equations. An extension to two-dimensional lattices is given by using Monte Carlo simulations, where TPD spectra are calculated. From those spectra we also obtain the remaining coverage in two-dimensional square lattice. The conclusions are presented in Section 4.

2. Rate equations in one-dimensional chain

Let us describe the kinetic of the process, following the evolution of a given configuration of particles in the line. For this purpose, it can be considered a system composed of a chain of M sites, where the state of each site can be either empty ($N_i = 0$) or occupied by a particle ($N_i = 1$). By using this notation, let us define the different steps of the process as follows:

(i) An incoming dimer is adsorbed with certain probability p_{ads}, if the pair of chosen neighboring sites are empty ($N_i = 0$ and $N_{i+1} = 0$);

(ii) dimer dissociate, with certain probability p_{dis} after adsorption;

(iii) eventually, diffusion of monomer units is allowed with certain jump rate Γ;

(iv) if two neighboring sites are occupied ($N_i = 1$ and $N_{i+1} = 1$), they react to form a dimer with certain probability p_{as};

(v) after that, desorption is attempted with probability p_{des} and the sites become empty (see Fig. 1). Particles interact each other with a coupling constant $J = \exp(-V/k_B T)$, where V is the interaction energy between two nearest-neighbor particles, k_B is the Boltzmann constant and T is the temperature. If either (or both) of the two sites is empty, the desorption attempt is rejected and the state of the sites remains unchanged.

In order to simplify the treatment, in the rest of the paper, $p_{dis} = p_{as} = 1$ and $\Gamma = 0$.

To describe the process, let us define $P(c;t)$ as the probability that the system is found in the configuration $c = \{N_1, N_2, \ldots, N_M\}$ at time t. The average occupation

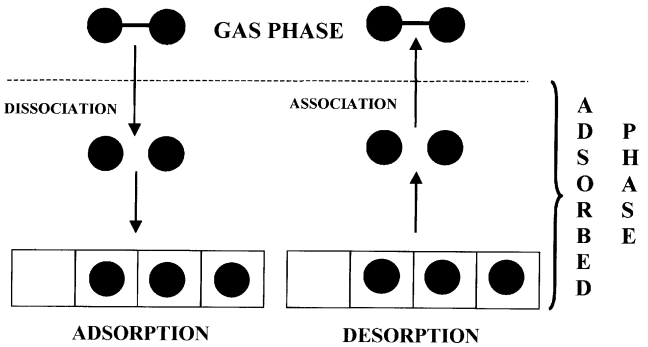

Fig. 1. Schematic representation of the adsorption–desorption process.

number or coverage θ is given by

$$\theta = \langle N \rangle = \frac{1}{M} \sum_i \sum_c N_i P(c;t) \,, \tag{1}$$

where the first sum runs over the sites "i" and the second one runs over all the microscopic configurations c. Higher moments are defined in the same way, as for example, the nearest-neighbor correlation σ,

$$\sigma = \langle NN \rangle = \frac{1}{M} \sum_i \sum_c N_i N_{i+1} P(c;t) \,. \tag{2}$$

The vacancy of the site "i" is defined as

$$E_i = (1 - N_i) \tag{3}$$

then its average is given by

$$\langle E \rangle = \frac{1}{M} \sum_i \sum_c (1 - N_i) P(c;t) \,. \tag{4}$$

Following the definition of the moments, there are a number of relations between them, for instance,

$$\langle NE \rangle = \langle N \rangle - \langle NN \rangle \,, \tag{5}$$

$$\langle NNE \rangle = \langle NN \rangle - \langle NNN \rangle \,, \tag{6}$$

$$\langle NEE \rangle = \langle NE \rangle - \langle NEN \rangle \,. \tag{7}$$

The evolution of the system can be followed through the time behavior of one generic site i. For this purpose a set of evolution rules, depending on the state of the site and its neighborhood, was built. After that, and properly averaging, a set of coupled differential equations are obtained. This technique has been used to analyze the irreversible growth models, particularly to derive the Langevin equations in $(1+1)$-dimensional systems [10] and dimer kinetics in one-dimensional lattice [11]. This method is particularly efficient in case where the use of master equation approach seems to be extremely difficult, if not impossible, specially in the irreversible growth models with quenched noise [12].

The method is rather simple and consists of monitoring the time evolution of a chosen site, through the following procedure: (i) A dummy index j is chosen and compared with the label of the site, if they are equal $i = j$, the trial continues, otherwise it is rejected. (ii) The occupation of a given site at time t_{n+1} is given by $N_i(t_{n+1})$ which depends on the state of the site at time t_n. This can be written as

$$N_i(t_{n+1}) = N_i(t_n) + G_{i,j}\,|_{ads} + G_{i,j}|_{des} \,, \tag{8}$$

where $G_{i,j}|_{ads}$ and $G_{i,j}|_{des}$ represent the local evolution rules for adsorption and desorption, respectively. Eq. (8), expresses that the occupation of the site i at time t_{n+1} depends on its value at time t_n modified by the adsorption or desorption of a given

dimer. The adsorption is considered as a Langmuir process, i.e., it is independent on the state of the neighborhood. Local evolution rule for adsorption is given by

$$G_{i,j}|_{ads} = [E_i E_{i+1}\delta_{i,j} + E_{i-1}E_i\delta_{i-1,j}]\Theta(p_{ads} - \xi_{ads}) , \tag{9}$$

where $\delta_{i,j}$ and $\delta_{i-1,j}$ are the Kronnecker delta. The step function $\Theta(p_{ads}-\xi_{ads})$ will be one, if the adsorption probability p_{ads} is greater than a random number ξ_{ads} ($p_{ads} > \xi_{ads}$), otherwise it will be zero. The function defined in Eq. (9) takes the value 1, if the pair of sites $i, i+1$ or $i-1, i$ are empty, the index j is equal to i or $i-1$, and the argument in the step function is positive, otherwise it is 0. (As is observed, p_{ads} does not depend on the occupation numbers of the nearest-neighbor of the dimer.)

For desorption the rule is defined as

$$\begin{aligned} G_{i,j}\,|_{des} = &-N_i N_{i+1}\delta_{i,j}\Theta(p_{des}(i-1, i+2) - \xi_{des}) \\ &-N_{i-1}N_i\delta_{i-1,j}\Theta(p_{des}(i-2, i+1) - \xi_{des}) . \end{aligned} \tag{10}$$

Here the function $G_{i,j}\,|_{des}$ takes the value -1, if the pair of sites $i, i+1$ or $i-1, i$ are occupied, the index j is equal to i or $i-1$ and the argument in the step function is positive, otherwise it is 0. The desorption probability $p_{des}(k,l)$ depends on the occupation numbers of the nearest-neighbor of the dimer and is defined as

$$p_{des}(k,l) = p^*_{des}\mathrm{e}^{-V/k_BT(N_k+N_l)} , \tag{11}$$

where p^*_{des} is a constant which does not depend on the occupation numbers.

To show how the method works, the evolution equation corresponding to the first moment (coverage) will be examplified. To do this let us introduce the following approximation:

$$\langle N_i(t_{n+1})\rangle - \langle N_i(t_n)\rangle \approx \tau_0 \frac{\mathrm{d}\langle N_i(t_n)\rangle}{\mathrm{d}t_n} \tag{12}$$

and setting $t = t_n$, the differential equation for $\langle N_i\rangle$ is obtained as,

$$\begin{aligned} \tau_0 \frac{\mathrm{d}\langle N_i\rangle}{\mathrm{d}t} = &\langle E_i E_{i+1}\delta_{i,j}\Theta_{ads}\rangle + \langle E_{i-1}E_i\delta_{i-1,j}\Theta_{ads}\rangle \\ &-\langle N_i N_{i+1}\delta_{i,j}\Theta(p_{des}(i-1, i+2) - \xi_{des})\rangle \\ &-\langle N_{i-1}N_i\delta_{i-1,j}\Theta(p_{des}(i-2, i+1) - \xi_{des})\rangle . \end{aligned} \tag{13}$$

After performing the products of the dynamic variables in the required sequence and taking the average on both sides, the equations of motion are constructed. To calculate the average appearing in the right-hand side of Eq. (12), one can take into account that some probabilities do not depend on the occupation variable, while others do depend, therefore the averages do not factorize in the same way. If the probabilities p_x for any x do not depend on the variable N_i or E_i and the randomly chosen numbers ξ are statistically independent, one can factorize the average as

$$\langle \Theta_x \delta_{k,j} m_i m_{i+1} \ldots m_k \ldots m_{i+r}\rangle = \langle \Theta_x\rangle\langle \delta_{k,j}\rangle\langle m_i m_{i+1}\ldots m_k \ldots m_{i+r}\rangle , \tag{14}$$

where $m_i = N_i$ or E_i and

$$\langle \Theta(p_x - \xi)\rangle = p_x \,, \tag{15}$$

$$\delta_{i,j} = 1/M \,. \tag{16}$$

If the probability p_x depends on N_k and /or E_k, the above factorization is not valid. To overcome the problem the next identity can be used,

$$\langle \Theta_x \delta_{k,j} m_i m_{i+1} \ldots m_k \ldots m_{i+r}\rangle = \langle \delta_{k,j}\rangle \langle p_x m_i m_{i+1} \ldots m_k \ldots m_{i+r}\rangle \,. \tag{17}$$

Using $\exp(N\alpha) = 1 + N[\exp(\alpha) - 1]$ for $N = 0, 1$ and the above ensemble average, the coupled evolution equations for the correlations are obtained. Then, the equation for the average occupation number is written as

$$\frac{\mathrm{d}\langle N\rangle}{\mathrm{d}t} = 2\,p_{ads}\langle EE\rangle - 2\,p^*_{des}[\langle NN\rangle + 2C\langle NNN\rangle + C^2\langle NNNN\rangle] \tag{18}$$

similarly for the nearest-neighbor correlation function,

$$\frac{\mathrm{d}\langle NN\rangle}{\mathrm{d}t} = p_{ads}[2\langle NEE\rangle + \langle EE\rangle] - p^*_{des}[\langle NN\rangle + (2+4C)\langle NNN\rangle) + C(2+3C)\langle NNNN\rangle] \,, \tag{19}$$

where $C = J - 1$.

To help the notation, the site indices of N and E are eliminated in the last two equations.

Otherwise, the adsorption and desorption probabilities must satisfy the following relation:

$$\frac{p_{ads}}{p^*_{des}} = \exp(-(\varepsilon_0 - \mu)/k_B T) \,. \tag{20}$$

In Eq. (20), μ is the chemical potential and ε_0 is the adsorption site energy which takes the value $\varepsilon_0 = 0$ in the rest of the paper.

Due to that the first two moments in Eqs. (18) and (19) depend on higher moments, a hierarchy of coupled differential equations is necessary to describe the kinetics of the process (equations for higher correlation functions are shown in the Appendix).

To obtain information from the set of coupled differential equations of motion, the hierarchy must be truncated. Several works have been written about closure approximations, particularly by ben-Avraham and Köhler [13], who have considered a mean-field (n,m)-cluster approximation for different lattice models. The simplest closure scheme is the Kirkwood approximation, in which one expresses all higher correlation functions in terms of two-body correlation functions. To develop a systematic closure scheme, one uses similar procedure as in equilibrium statistical mechanics. For instance, in the quasi-chemical approximation, which gives exact results in one dimensional space, one calculates the partition function for two sites exactly and then distributes these pairs randomly over the lattice. Therefore, for the reversible kinetics, where the adsorbed phase is in equilibrium with the gas phase, a (2,1) Kirkwood closure is enough to obtain the exact solution for the coverage and nearest-neighbors correlation function. This scheme can be used also in the irreversible desorption without lateral interactions.

However, in the presence of lateral interactions, the (2,1) closure fails and more accurate closure is necessary. In fact, one observes that a (4,3) Kirkwood closure gives an exact solution for irreversible desorption and also for thermal desorption. This arises because in order to desorb a given particle, one needs to know its local environment. This effect was also observed in the desorption of monomers [14] and dimers [11] where (3,2) and (4,3) closures were used, respectively.

3. Analysis of the results

3.1. Reversible kinetics. Equilibrium

To derive the equilibrium properties from the kinetics, it is necessary to reduce the dimension of the set of coupled differential equations. To this purpose, a (2,1) Kirkwood closure to obtain the coverage and nearest-neighbor correlation function in exact form has been used. This scheme is equivalent to the quasi-chemical solution, which is exact in one-dimensional space.

After truncating the hierarchy of differential equations, a set two coupled equations is obtained for the coverage and nearest-neighbors correlation function, respectively. Equating to zero both equations, we obtain the following expression for the coverage,

$$\exp(\mu/k_B T) = \frac{\langle NN\rangle(1+C)[\theta^2 + C\langle NN\rangle(2\theta-1)]}{\theta^2[1-2\theta+\langle NN\rangle]} \tag{21}$$

where the nearest-neighbors correlation function is given by

$$\langle NN\rangle = \frac{2C\theta - 1 - C + \sqrt{C^2(1-2\theta)^2 + C(2-4\theta+4\theta^2)+1}}{2C}\,. \tag{22}$$

For, $C = 0$, one can obtain

$$\exp(\mu/k_{BT}) = \frac{\theta^2}{(1-\theta)^2} \tag{23}$$

with

$$\langle NN\rangle = \theta^2\,. \tag{24}$$

The isotherms given by Eqs. (21) and (23) are valid only for the case where the dimers dissociate instantaneously after adsorption, and desorption proceeds from two random neighboring monomer units which can or cannot belong to the original dimer.

In order to analyze the behavior of the adsorption process as a function of lateral interaction, in Fig. 2, a set of adsorption isotherms for different values of V is plotted. As is observed, the isotherms are very different from the corresponding to dimer adsorption [11]. In fact, for low values of chemical potential, adsorption for repulsive interactions is higher than for attractive interactions. To understand such a situation, it is necessary to highlight that adsorption is defined as a Langmuir process, that is, the probability of adsorption does not depend on the neighborhood of a pair of sites, therefore, the equilibrium coverage depends on the desorption process.

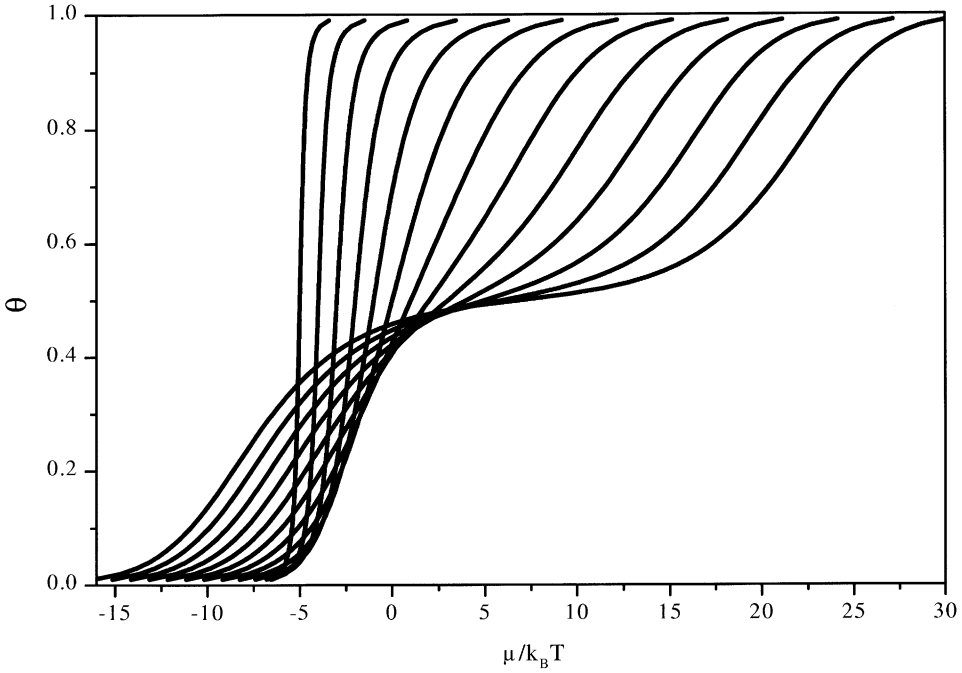

Fig. 2. Adsorption isotherms, $V/k_BT = 5, 4, 3, 2, 1, 0, -1, -2, -3, -4, -5, -6, -7$ (left to right at $\theta = 0.8$).

Let us consider four consecutive occupied sites limited by empty sites; in case of attractive lateral interactions, the desorption probability is lower for the dimer in the middle of the configuration than those located in the extreme of the chain, consequently after reactions, all the particles are desorbed. For repulsive lateral interactions, desorption probability is higher for the dimer located in the middle of the configuration than those located in the extremes; then only one dimer desorbs and two monomers remain adsorbed.

Another relevant feature observed for repulsive lateral interactions is the classical step at half coverage which appears for repulsive lateral interactions. Note that, in our case, the alternation between particles and vacancy cannot be perfect, because contacts between particles are necessary in order to have desorption.

3.2. Irreversible kinetics. Isothermal desorption and remaining coverage

In the following, the desorption kinetics is analyzed, in particular the isothermal process. After truncating the hierarchy system and neglecting adsorption, we obtain the time dependence of the coverage and correlation functions solving the following two equations:

$$\frac{\mathrm{d}\theta}{\mathrm{d}t} = -p^*_{des}\left[2\sigma + 4C\,\frac{\sigma^2}{\theta} + 2C^2\,\frac{\sigma^3}{\theta^2}\right] \tag{25}$$

and

$$\frac{d\sigma}{dt} = -p^*_{des}\left[\sigma + (2+4C)\frac{\sigma^2}{\theta} + C(2+3C)\frac{\sigma^3}{\theta^2}\right], \tag{26}$$

where we replaced $\langle N\rangle = \theta$ and $\langle NN\rangle = \sigma$ in order to simplify the notation.

In particular, for the case without lateral interactions $C = 0$, the solution is given by

$$\theta = \theta_0 \exp[2\theta_0(e^{-p^*_{des}t} - 1)] \tag{27}$$

and

$$\sigma = \theta_0^2 \exp[2\theta_0(e^{-p^*_{des}t} - 1) - p^*_{des}t], \tag{28}$$

where θ_0 is the initial coverage. In the limit $t \to \infty$ we obtain the remaining coverage, θ_R as a function of the initial coverage,

$$\theta_R = \theta_0 \exp(-2\theta_0). \tag{29}$$

Particularly, for $\theta_0 = 1$, we can relate this remaining coverage with the jamming coverage in the classical one-dimensional RSA problem [15], considering that the desorption of dimer is equivalent to the random sequential adsorption of two adjacent vacancy. In fact,

$$\theta_J = (1 - \theta_R) \simeq (1 - e^{-1}). \tag{30}$$

To analyze the dependence of the remaining coverage with the lateral interaction, it is necessary to solve the seven coupled differential equations, (18), (19), (31)–(35), after using (4,3) Kirkwood closure and neglecting adsorption. In Fig. 3 the remaining coverage as a function of the initial coverage θ_0 has been plotted, for different lateral interactions. The initial coverage corresponds to the equilibrium configuration. As is observed, there are two set of curves depending on the sign of V: (i) the attractive lateral interaction, where the remaining coverage is always smaller than for $V = 0$ (filled line) and (ii) repulsive lateral interaction, where θ_R is always greater than the non-interacting case. The explanation of both cases is straightforward: attraction favors the contact between monomer units and then the desorption of dimers is higher, repulsive interaction does not contribute to the contact and therefore desorption diminished. For very high values of repulsive interaction, desorption starts for initial coverage higher than $\theta_0 > 0.5$.

3.3. Thermal desorption

In this section, the thermal desorption kinetics is presented, particularly the thermal desorption spectra in one and two-dimensional lattices are analyzed. The first case will be studied solving the kinetics equations, the second one, by using Monte Carlo simulations. The TPD spectra for immobile desorption in 1D lattice are also obtained by solving Eqs. (18), (19) and (31)–(35), where adsorption process is neglected.

In Fig. 4(a), the TPD spectra for non-interacting immobile adsorbate in a one-dimensional chain have been plotted. In all desorption experiments the rate of desorption is proportional to the number of possible pairs in the surface; for this reason,

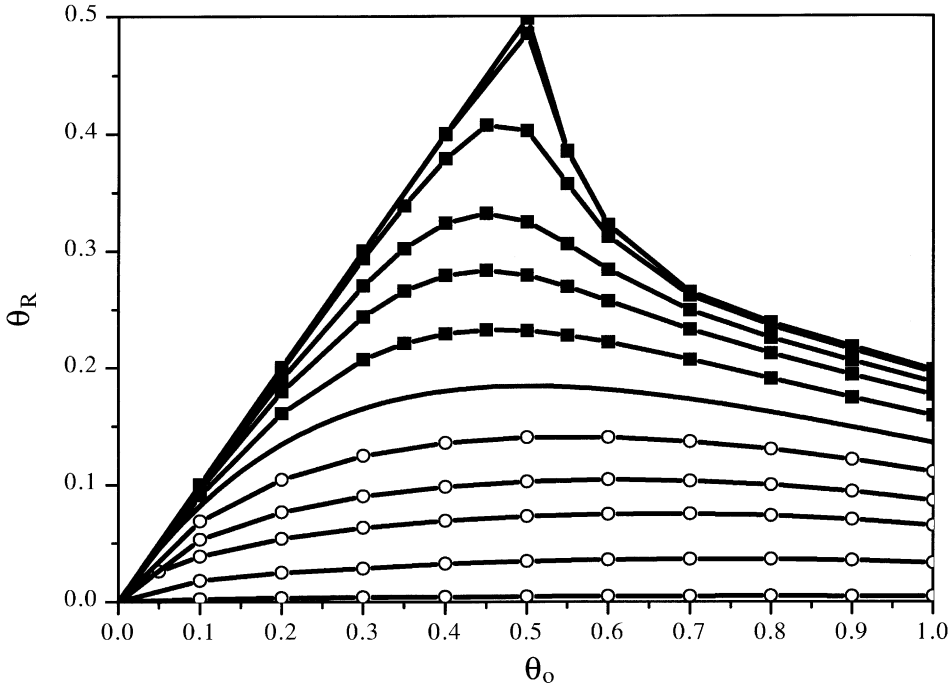

Fig. 3. Isothermal remaining coverage as a function of the initial coverage. V(kcal/mol) $= -1.5, -1, -0.5, -0.3, -0.2, -0.1, 0, 0.1, 0.2, 0.3, 0.5, 1$ (top to bottom). In the desorption experiment the temperature was $T_0 = 60$ K.

the curves are slightly shifted to the right as the initial coverage diminishes. It is important to note that, in all cases, the initial configuration corresponds to the equilibrium configuration.

In Fig. 4(b), the spectra for attractive lateral interaction have been shown. The position of the maximum is almost independent of the initial coverage; this is due to the fact that dimers desorb from the extreme of the monomer domains.

In Fig. 4(c), the desorption curves for repulsive lateral interactions have been plotted. Due to the repulsion, there are three possible cases for a generic dimer in the line: (i) with two neighbors (very unstable), (ii) with only one neighbor (unstable) and (iii) isolated (indistinct). In this figure, we can observe three peaks for $\theta_0 > 0.5$. The first peak corresponds to case (i) the second to case (ii), and finally the third to the case (iii). For lower initial coverage only the case (ii) and (iii) are present.

The two-dimensional TPD spectra for non- and attractive lateral interactions are very similar to the one-dimensional case. The repulsive case, however, is more interesting. In fact, in Fig. 5, the TPD spectra for three different repulsive interactions are plotted. Case (i), for $V = -0.2$ kcal/mol, see Fig. 5(a); the maximum was shifted to higher temperature as the initial coverage diminished. However, two well different regime according to the value of θ_0 can be distinguished. In fact, for $\theta_0 \leqslant 0.4$ the temperature

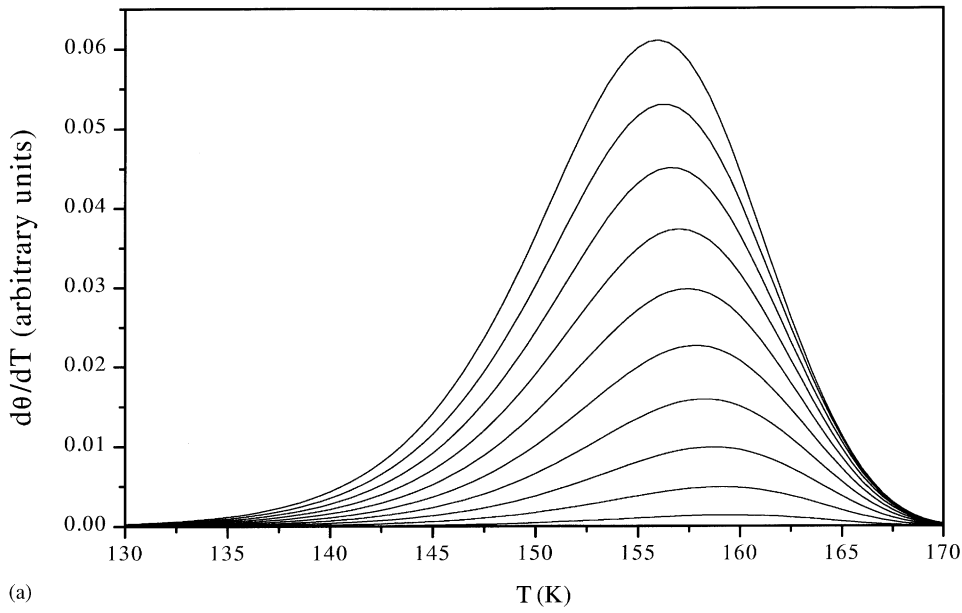

(a)

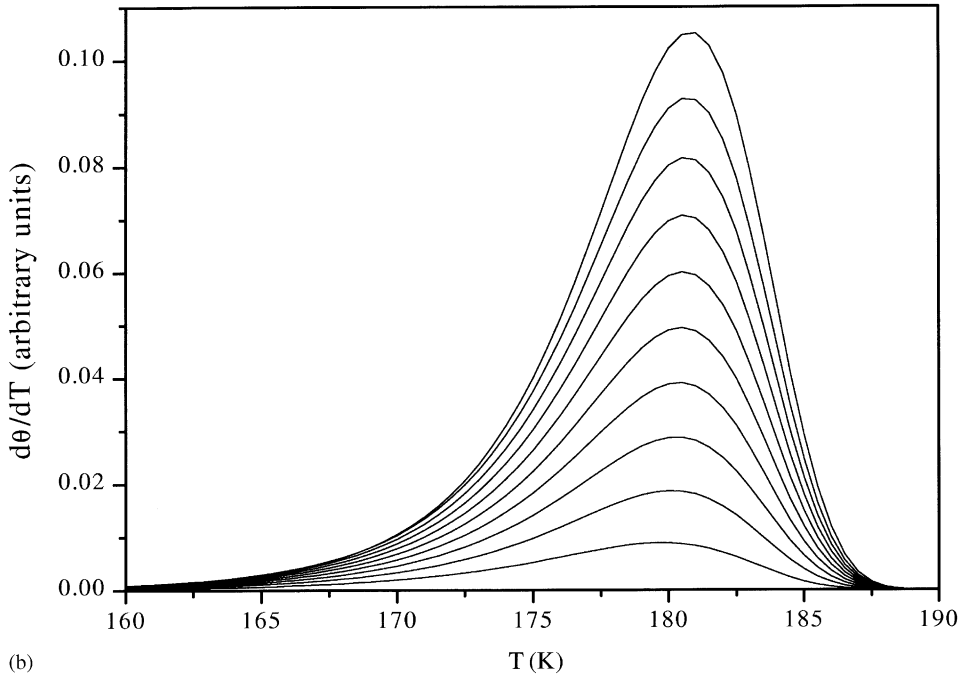

(b)

Fig. 4. TPD spectra in one-dimensional lattice for different initial coverage. (a) No interaction, (b) attractive interaction (1 kcal/mol) and (c) repulsive interaction (−1 kcal/mol). The initial coverage for the cases (a) and (b) increase from $\theta_0 = 0.1$ to 1 in step of 0.1, while for the case (c) increase from $\theta_0 = 0.5$ to 1 in step of 0.05.

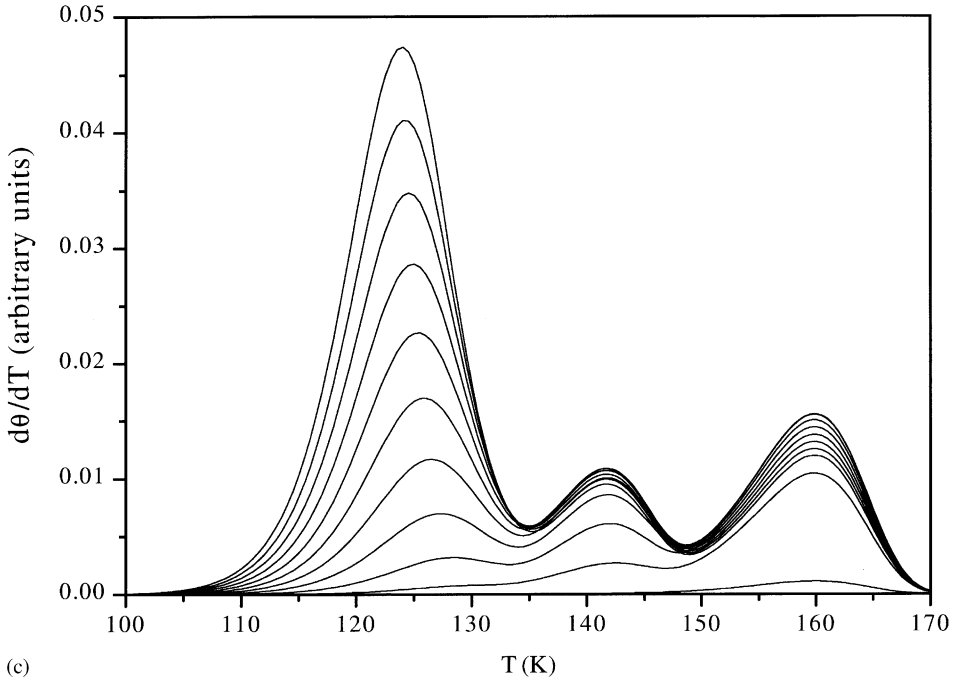

Fig. 4. Continued.

of the maximum is almost constant, while for $\theta_0 > 0.4$ this temperature diminished almost linearly. To visualize this fact, it has been plotted in Fig. 6, the temperature of the highest peak as a function of the initial coverage for different lateral interactions. Case (ii): for $V = -0.3$ kcal/mol, see Fig. 5(b): There are three desorption regimes, the first one, for $\theta_0 \leqslant 0.45$ where the temperature of the peak is almost constant, the second regime, for $0.5 \leqslant \theta_0 \leqslant 0.65$ where the temperature is also constant but lower, and finally for $\theta_0 > 0.65$ the temperature of the peak diminished as a function of the initial coverage. Case (iii): for $V = -0.5$ kcal/mol, see Fig. 5(c), and for $\theta_0 < 0.5$ there is no desorption. For $0.5 < \theta_0 \leqslant 0.65$ the temperature of the maximum is almost constant and for $\theta_0 > 0.65$ the temperature diminished with θ_0.

To explain the behavior of the spectra, let us describe the initial configuration for the desorption experiment as a function of lateral interaction. All the spectra are obtained starting the desorption at initial temperature $T_0 = 60$ K. The initial configuration, which is the equilibrium configuration, depends on the lateral interaction. This is due to the fact that for temperature below the critical one $T < T_c$, the adsorbate undergoes an order disorder phase transition, where at half coverage the particles are located in a chessboard-like structure due to the repulsion between nearest neighbors; this structure is called $c(2 \times 2)$ ordered phase. The critical temperature at half coverage is exactly calculated and is given by the following relation, $k_B T_c/V = 0.56729\ldots$ [16], which depends on the lateral interaction. The phase diagram [17] corresponding to this kind

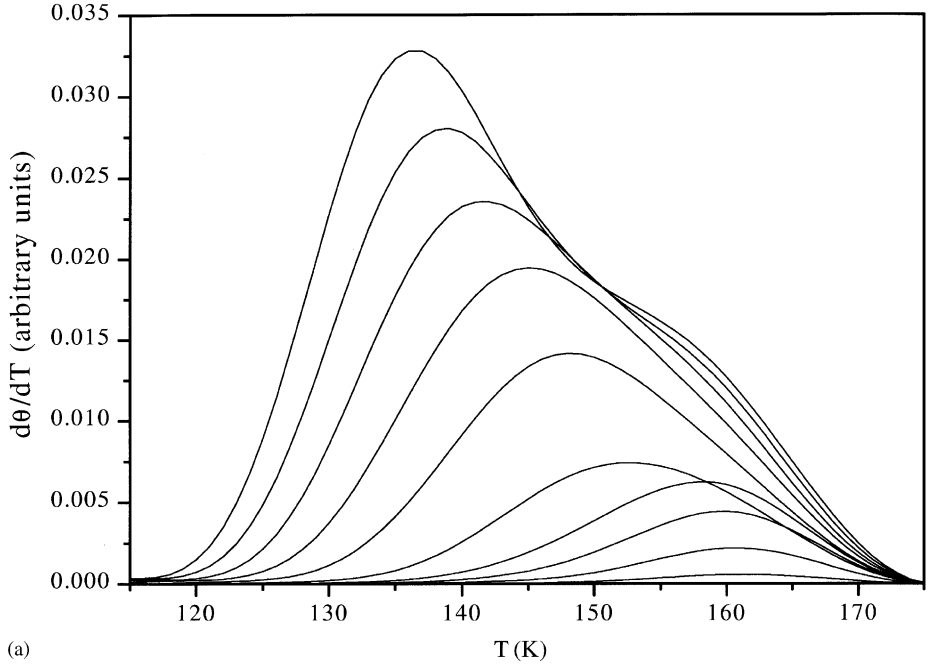

(a)

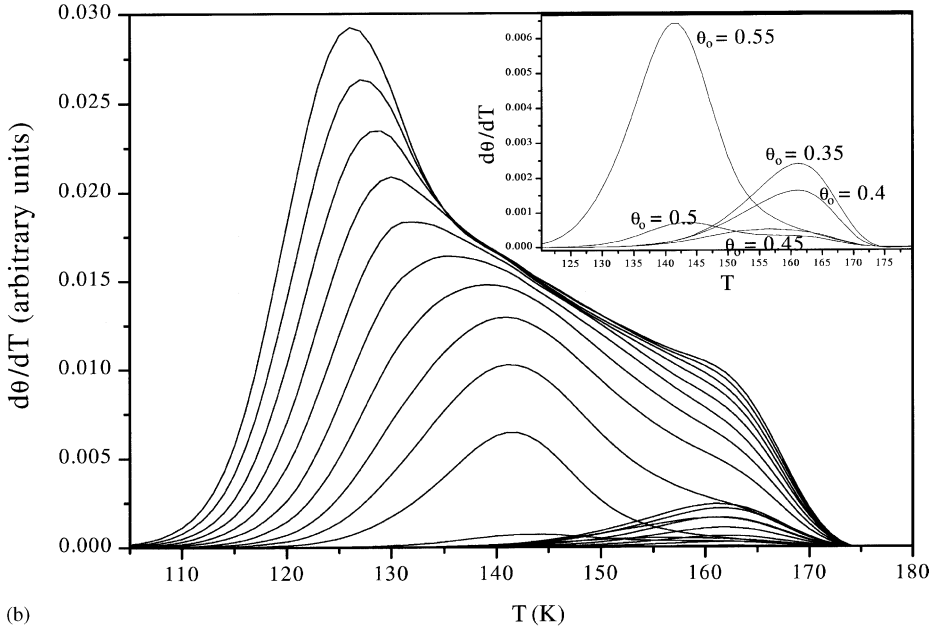

(b)

Fig. 5. TPD spectra in two-dimensional lattice for different values of repulsive interaction: (a) $V = -0.2$ kcal/mol, with initial coverage varying from $\theta_0 = 0.1$ to 1 in step of 0.1; (b) $V = -0.3$ kcal/mol, with initial coverage at $T = 130$ K, varying from $\theta_0 = 1$ to 0.5 in step of 0.05 (top to bottom); (c) $V = -0.5$ kcal/mol, with $\theta_0 = 0.55$ to 1 in step of 0.05.

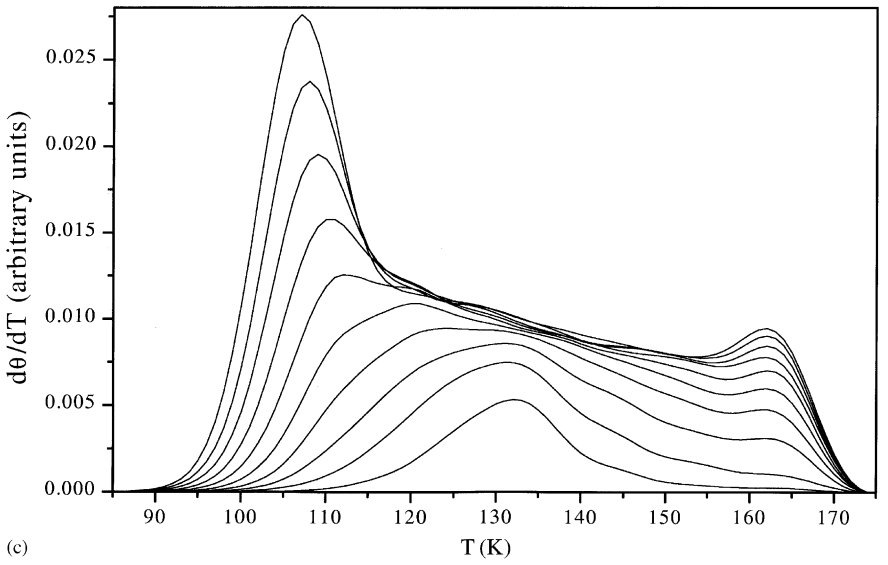

Fig. 5. Continued.

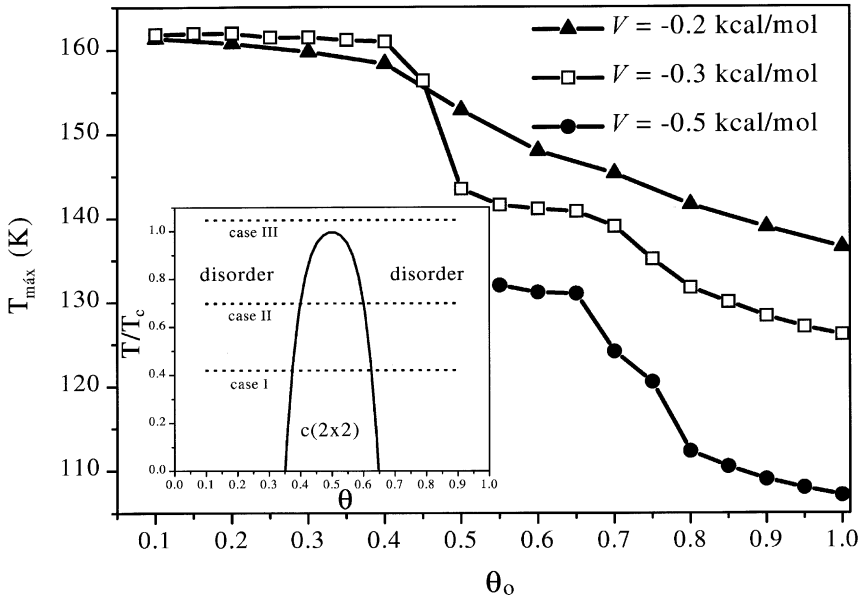

Fig. 6. Temperature of the maximum for the TPD spectra as a function of initial coverage. In the inset, the phase diagram for monomers with nearest-neighbor repulsive interaction is shown.

of continuous phase transitions is showed in the inset of Fig. 6, the horizontal lines correspond to the relative temperature of the initial configuration used in the desorption experiment. Note that the initial configuration is obtained after reaching the thermodynamic equilibrium. By using this argument the spectra can be discussed: In case (i) the critical temperature at half coverage is $T_c = 57.30$ K and the relative value $T_c/T_0 = 1.047$, therefore, all the initial configurations are disordered, irrespective of the initial coverage. In other words, particles are distributed randomly in the surface. Then, for $0.5 < \theta_0 < 1$ the number of nearest neighbors diminished almost linearly with the initial coverage due to the repulsion and the corresponding maximum is shifted to higher temperature. For coverage $0 < \theta_0 < 0.5$, the contact is less significant, therefore the maximum is almost independent of the coverage. In case (ii), the critical temperature at half coverage is $T_c = 85.95$ K and their relative value $T_c/T_0 = 0.698$. There are three possible cases, for $0.6 < \theta_0 < 1$ the initial configuration is disordered, then the spectra behave as is described above. Additionally, the shoulder appearing for higher values of initial coverage corresponds to those isolated dimers. For $0.4 < \theta_0 < 0.6$, the initial configurations are ordered, then two possibilities must be distinguished: (a) if the $\theta_0 > 0.5$ the dimers, which desorb, interact on the average with three occupied nearest neighbors, irrespective of the initial coverage; (b) if $\theta_0 < 0.5$, due to the order, there is no contact between monomers in the arrangement and consequently there is no desorption. Finally, for $\theta_0 < 0.4$ the initial configurations are out of the phase diagram, and then desorption is higher than for values of θ_0 belonging to the ordered phase. For larger interactions (case (iii)), the critical temperature at half coverage is $T_c = 143.25$ K and the relative value $T_c/T_0 = 0.4188$. The spectra corresponding to the initial coverage $\theta_0 > 0.625$ are similar to the later case, however the shoulder that appears at high temperature becomes peak in a second. For coverage $\theta_0 < 0.625$ the initial configurations are ordered; finally for $\theta_0 < 0.5$ there is not desorption.

Finally, the remaining coverage from the thermal desorption spectra is studied. In fact, for a given initial coverage, and after the desorption experiment, it is observed that the total area under the desorption curve is less than the initial coverage; that is because the adsorbed phase is completely immobile and some particles do not react during the process. This method allows the calculation of the remaining coverage in a more efficient way than under isothermal conditions. In Fig. 7(a), it has been plotted, the thermal remaining coverage as a function of initial coverage for a one-dimensional lattice, for different interactions. The behavior of the curves are similar to those obtained under isothermal conditions (Fig. 3). The thermal remaining coverage for a two-dimensional square lattice is shown in Fig. 7(b); there is some difference in the one-dimensional lattice, especially for repulsive interactions, where the effect of the order is visualized in particular for strong repulsive interactions.

4. Conclusions

In this paper the kinetics of dissociative adsorption followed by associative desorption has been studied. To obtain the kinetic equations, the so-called local evolution rules have been used, which are alternative to the master equation approach.

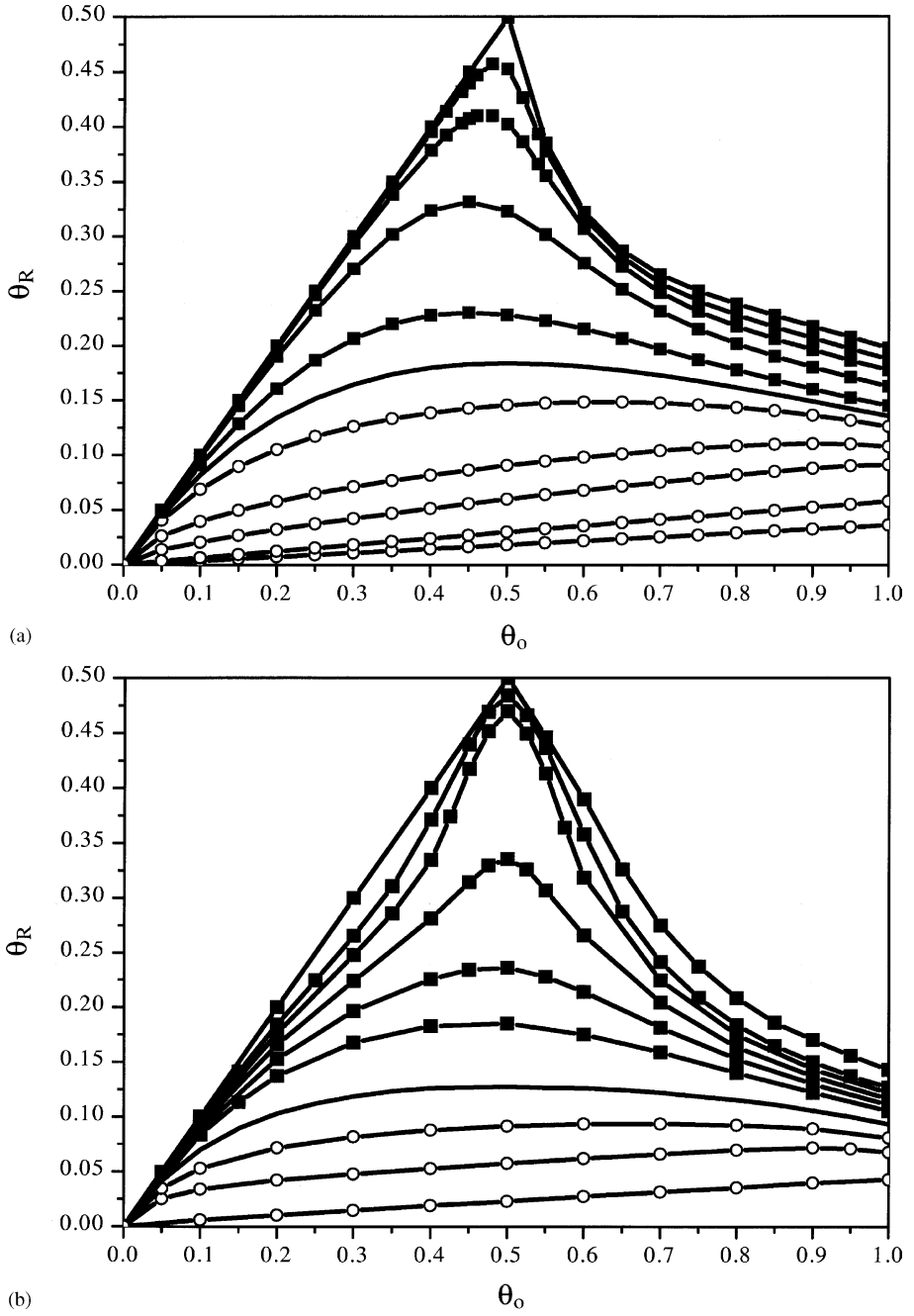

Fig. 7. Thermal remaining coverage as a function of the initial coverage. In the desorption experiment the initial temperature was $T_0 = 60$ K. (a) for one-dimensional lattice V(kcal/mol) $= -1.7, -0.7, -0.5, -0.3, -0.1, 0, 0.1, 0.3, 0.5, 1, 1.5$ (top to bottom); (b) for two-dimensional square lattice. V(kcal/mol) $= -0.5, -0.3, -0.25, -0.2, -0.15, -0.1, 0, 0.1, 0.2, 0.4$ (top to bottom).

The system of coupled differential equations is truncated by using a mean-field (n,m)-cluster approximation with different degree of accuracy.

To obtain the equilibrium properties from the kinetic equations, a (2,1) closure has been used. As a result, the coupled differential equations for the coverage and the nearest-neighbor correlation functions that correspond to the quasi-chemical solution is obtained, which is exact in one-dimensional space. In the adsorption isotherms it is observed that at coverage $\theta < 0.5$, and the repulsive lateral interaction increases adsorption with respect to the attractive case. The exact expression for the isotherm differs from the corresponding to the non-dissociative dimer adsorption.

The non-equilibrium kinetics is also analyzed, with the focus on irreversible desorption. After desorption of nearest-neighbor monomers, a remaining coverage results from isolated monomers, provided that the adsorbate mobility is neglected. The exact solution for one-dimensional case is reported. As discussed above, the analytical expression for the non-interacting case is related with the classical RSA dimer model. However, the interacting case corresponds to a new jamming state in the line.

The thermal desorption spectra are also obtained from the kinetic equations. The effect of the lateral interactions on the TPD spectra is presented. By using MC simulation the study is extended to the two-dimensional case. The effect of the lateral interactions is also studied. The most interesting case appears for repulsive lateral interactions in the 2D case, where the kinetics are strongly dependent on the initial temperature and coverage, especially for the configurations belonging to the ordered region of the phase diagram.

It is important to emphasize that the local evolution rules, which have been used here, present advantages compared with other methods like the master equation approach. In fact, even when the equation for the evolution of a given state looks complicated, the derivation is rather simple and can be easily implemented by symbolic language. In addition, the definition of the Hamiltonian of the system is not necessary, as in the master equation approach. Furthermore, other mechanisms can be added to the kinetic process, as more complex surface reactions, surface reconstruction, etc.

Acknowledgements

This work is partially supported by the CONICET (Argentina). The authors want to thank A. Boscoboinik for reading the manuscript (Argentina).

Appendix

The coupled differential equations for the third- and fourth-order correlation functions is presented, which are necessary to obtain the desorption kinetics:

$$\frac{\mathrm{d}\langle NNN\rangle}{\mathrm{d}t} = 2\,p_{ads}[\langle NNEE\rangle + \langle NEE\rangle] - 2\,p^{*}_{des}(1+C)[\langle NNN\rangle + (1+C)\langle NNNN\rangle + C\langle NNNNN\rangle]\,, \qquad (31)$$

$$\frac{\mathrm{d}\langle NEN\rangle}{\mathrm{d}t} = 2\,p_{ads}\langle NEEE\rangle - 2\,p^{*}_{des}[\langle NENN\rangle + C\langle NNNEN\rangle]\,, \tag{32}$$

$$\begin{aligned}\frac{\mathrm{d}\langle NNNN\rangle}{\mathrm{d}t} &= p_{ads}[2\langle NNNEE\rangle + 2\langle NNEE\rangle + \langle NEEN\rangle] \\ &\quad - p^{*}_{des}(1+C)[(3+C)\langle NNNN\rangle \\ &\quad + 2(1+C)\langle NNNNN\rangle + 2C\langle NNNNNN\rangle]\,,\end{aligned} \tag{33}$$

$$\begin{aligned}\frac{\mathrm{d}\langle NEEN\rangle}{\mathrm{d}t} &= p_{ads}[2\langle NEEEE\rangle - \langle NEEN\rangle] \\ &\quad - p^{*}_{des}[2\langle NNEEN\rangle + 2C\langle NNNEEN\rangle \\ &\quad - (1+C)^{2}\langle NNNN\rangle]\end{aligned} \tag{34}$$

and

$$\begin{aligned}\frac{\mathrm{d}\langle NENN\rangle}{\mathrm{d}t} &= p_{ads}[\langle NNEEE\rangle + \langle NENEE\rangle + \langle NEEE\rangle] \\ &\quad - p^{*}_{des}[\langle NNENN\rangle + C\langle NNNENN\rangle \\ &\quad + (1+C)\langle NENNN\rangle + C(1+C)\langle NENNNN\rangle]\,.\end{aligned} \tag{35}$$

References

[1] R.B. Anderson, P.T. Dawson (Eds.), Experimental Methods in Catalytic Research, Vols. I–III, Academic Press, New York, 1976.
[2] P.R. Norton, in: D.A. King, D.P. Woodruff (Eds.), Chemical Physics of Solid Surfaces and Heterogeneous Catalysis, Vol. 4, Elsevier, Amsterdam, 1982, p. 27.
[3] V.P. Zhdanov, Elementary Physicochemical Processes on Solid Surfaces, Plenum Press, New York, 1991.
[4] E.V. Albano, HCR Adv. Ed. Rev. 3 (1996) 389.
[5] A. Cassuto, D.A. King, Surf. Sci. 102 (1981) 388.
[6] V.P. Zhdanov, B. Kasemo, Chem. Phys. 177 (1993) 519, and reference therein.
[7] R.D. Levine, G.A. Somorjai, Surf. Sci. 232 (1990) 407.
[8] F. Nieto, J.L. Riccardo, G. Zgrablich, Langmuir 9 (1993) 2504.
[9] F. Nieto, A.P. Velasco, J.L. Riccardo, G. Zgrablich, Surf. Sci. 315 (1994) 185.
[10] G. Costanza, Phys. Rev. E 55 (1997) 6501;
G. Costanza, J. Phys. A: Math. Gen. 31 (1998) 7211.
[11] G. Costanza, S. Manzi, V.D. Pereyra, Surf. Sci. 524 (2003) 89.
[12] G. Costanza, Physica A 330 (2003) 421.
[13] D. ben Avraham, J. Köhler, Phys. Rev. A 45 (1992) 8358.
[14] J.W. Evans, D.K. Hoffman, H. Pak, Surf. Sci. 192 (1987) 475.
[15] J.W. Evans, Rev. Mod. Phys. 65 (4) (1993) 1281, and reference therein.
[16] B.M. Mc Coy, T.T. Wu, The two-dimensional Ising Model, Harvard University Press, Cambridge, MA, 1973.
[17] K. Binder, D.P. Landau, Phys. Rev. B 21 (1980) 1941.